Electron-Phonon Interactions and Excitonic Dephasing in Semiconductor Nanocrystals

T. Takagahara
NTT Basic Research Laboratories, Musashino-shi, Tokyo 180, Japan
(Received 24 May 1993)

The size dependence of the contribution to the excitonic dephasing rate in semiconductor nanocrystals is clarified for various electron-phonon coupling mechanisms. On the basis of these dependencies, the commonly observed linearly temperature-dependent term of the excitonic dephasing rate and the proportionality of its magnitude to the inverse square of the nanocrystal size are attributed to pure dephasing due to deformation-potential coupling. The calculated coefficients of the linearly temperature-dependent term are quantitatively in good agreement with the experimental results on CdSe and CuCl nanocrystals.

PACS numbers: 78.66.Li, 71.35.+z, 73.20.Dx

Semiconductor nanocrystals of a size comparable to or smaller than the exciton Bohr radius in bulk material are attracting much attention from the fundamental physics viewpoint and from the interest in the application to functional devices. Especially their novel optical properties due to the discrete electronic energy levels have been investigated extensively [1,2]. In semiconductor nanocrystals, not only the electronic energy levels but also the lattice vibrational modes become discrete due to the three-dimensional confinement. The consequences of the latter feature, namely, the phonon confinement, are now being studied extensively. The longitudinal optical (LO) phonons in semiconductor nanocrystals were observed by the resonance Raman scattering [3–5] and the size dependence of the electron–LO-phonon coupling strength was discussed [4]. Also the size-quantized acoustic phonon modes were observed by the low-frequency Raman scattering [6].

Recently, in addition to these studies, the excitonic dephasing in various semiconductor nanocrystals has been measured as a function of nanocrystal size and temperature. In CuCl nanocrystals, the homogeneous linewidth of the excitonic transition was measured from the luminescence linewidth under size-selective excitation [7] and by spectral hole burning [8]. In nanocrystals of II-VI compounds, the excitonic dephasing constant was measured by spectral hole burning [9–12] and by four-wave mixing [13,14]. The commonly observed T- (temperature-) linear behavior of the excitonic dephasing rate suggests the importance of the electron-phonon interaction with acoustic phonon modes, although the relevant temperature range is dependent on the nanocrystal size and the material. In the higher temperature region, the temperature dependence of the excitonic dephasing rate deviates from the T-linear behavior, indicating the participation of LO phonons.

In this Letter, we derive electron-phonon interactions with acoustic phonons in semiconductor nanocrystals and clarify the size dependence of the contribution to the excitonic dephasing rate for various electron-phonon coupling mechanisms, i.e., the deformation-potential coupling and the piezoelectric coupling. On the basis of these results, we identify the origin of the commonly observed T-linear term of the excitonic dephasing rate and of the proportionality of its magnitude to the inverse square of the nanocrystal size.

In order to derive the electron-phonon interaction, we must first specify the acoustic phonon modes in semiconductor nanocrystals. As long as the nanocrystal size is not too small, its acoustic properties can be described in terms of the elastic vibration of a homogeneous particle. In the following, the shape of a nanocrystal is assumed to be spherical and the anisotropy of the elastic constants is neglected for simplicity of the arguments. Then the vibrations of an elastically isotropic sphere can be described by

$$\rho\frac{\partial^2}{\partial t^2}u=(\lambda+\mu)\mathrm{grad}\,\mathrm{div}\mathbf{u}+\mu\nabla^2\mathbf{u}\,, \tag{1}$$

where $\mathbf{u}$ is the lattice displacement vector, ρ is the mass density, and λ and μ are the Lame's constants [15]. The eigenmodes of the above equation under the stress-free boundary condition were studied by Lamb for the first time [16]. There are two kinds of eigenmodes, namely, torsional modes and spheroidal modes. The former modes are purely transversal, whereas the latter ones are mixed modes of transverse and longitudinal characters.

The electron-phonon interaction with acoustic phonon modes arises mainly through the deformation-potential coupling and the piezoelectric coupling. Although the detailed form of the deformation-potential coupling is dependent on the crystal symmetry [17], the most dominant term can be described by $E_d\,\mathrm{div}\mathbf{u}$, where E_d is the deformation potential. Hereafter only this term will be taken into account. The torsional modes do not contribute to this coupling because of their transversal character.

In the polar semiconductors, the lattice strain produces the lattice polarization and this polarization interacts with an electron. The lattice polarization is given in the Cartesian coordinates as $\mathbf{P}_{PZ}(\mathbf{r})=(e_{15}e_{zx},e_{15}e_{yz},e_{31}(e_{xx}+e_{yy})+e_{33}e_{zz})$ for the wurtzite structure and as $\mathbf{P}_{PZ}(\mathbf{r})=e_{14}(e_{yz},e_{zx},e_{xy})$ for the zinc blende structure, respec-

tively, where e_{ij} is the strain tensor and e_{15}, e_{31}, e_{33}, and e_{14} are the piezoelectric constants [18]. The electron-lattice interaction is given by the potential energy of the lattice polarization in the electric field induced by an electron and is represented as

$$-\frac{e}{\epsilon}\int d^3\mathbf{r}\nabla_{\mathbf{r}}\left(\frac{1}{|\mathbf{r}-\mathbf{r}_e|}\right)\cdot\mathbf{P}_{\mathrm{PZ}}(\mathbf{r})=\sum_{l_e,m_e,l,m,j}\mathcal{P}_{l_e,m_e,l,m,j}(r_e)Y_{l_e,m_e}(\Omega_e)[b_{l,m,j}+(-1)^m b^{\dagger}_{l,-m,j}]\,, \tag{2}$$

where (r_e,Ω_e) denotes the position of an electron in the spherical coordinates, $-e$ the electron charge, ϵ the dielectric constant, $Y_{l,m}$ a spherical harmonic, and b ($b^{\dagger}$) is the annihilation (creation) operator of the phonon mode with the angular momentum indices (l,m) and the radial quantum number j. The explicit expressions of $\mathcal{P}_{l_e,m_e,l,m,j}$ are too lengthy to be given here.

It is very important to examine the size dependence of these electron-phonon interactions in order to understand the mechanisms of the excitonic dephasing. In the case of the deformation-potential coupling, the size dependence arises from div$\mathbf{u}$ and can be estimated as

$$\mathrm{div}\mathbf{u}\propto\frac{1}{R}\frac{1}{\sqrt{R^3}}\frac{1}{\sqrt{\omega}}\sim\frac{1}{R^2}\,, \tag{3}$$

where R is the radius of a spherical nanocrystal and the first factor comes from the operation of div, the middle one from the normalization of the phonon mode, and the third one comes from the quantization of the phonon mode. The eigenfrequency ω of (1) is given by $(\lambda+2\mu)h^2=\rho\omega^2$ or $\mu k^2=\rho\omega^2$, where h and k are determined by the boundary conditions [15] and scale as $1/R$. Thus the eigenfrequency ω scales as $1/R$ and we obtain the dependence in (3).

In the case of the piezoelectric coupling, the strain tensor has the same size dependence as div$\mathbf{u}$, namely, $1/R^2$ and we obtain

$$\int d^3\mathbf{r}\nabla\left(\frac{1}{|\mathbf{r}-\mathbf{r}_e|}\right)\cdot\mathbf{P}_{\mathrm{PZ}}(\mathbf{r})\propto R^3\frac{1}{R^2}\frac{1}{R^2}\sim\frac{1}{R}\,, \tag{4}$$

where the first factor comes from the volume integral, the middle one from $\nabla(1/|\mathbf{r}-\mathbf{r}_e|)$, and the third one comes from the piezoelectric polarization $\mathbf{P}_{\mathrm{PZ}}(\mathbf{r})$. From these size dependencies, we see that in the small size region the deformation-potential coupling is dominant, whereas in the large size region the piezoelectric coupling becomes dominant.

Now that the electron-phonon interactions in semiconductor nanocrystals are derived, we can calculate the excitonic dephasing constant. The excitonic dephasing rate is the decay rate of the excitonic polarization and in general consists of the pure (adiabatic) dephasing constant and a half of the longitudinal decay constant. The former part arises from the fluctuation of the excitonic energy due to the virtual emission and absorption of phonons without the change of the excitonic state, whereas the latter part comes from the phonon-assisted transitions of the relevant excitonic state to other excitonic states. In other words, the diagonal and off-diagonal matrix elements of the electron-phonon interaction with respect to the excitonic states are responsible to the former and latter parts of the dephasing rate, respectively. When specified to the electronic ground state $|g\rangle$ and the lowest excitonic state $|\mathrm{ex}\rangle$, the diagonal part of the relevant Hamiltonian in the Franck-Condon approximation can be written as

$$H=|g\rangle\sum_j\hbar\omega_j b_j^{\dagger}b_j\langle g|+|\mathrm{ex}\rangle\sum_j[\hbar\omega_j b_j^{\dagger}b_j+\gamma_j(b_j+b_j^{\dagger})]\langle\mathrm{ex}|\,, \tag{5}$$

where the subscript j is the phonon mode index, and ω_j is the mode frequency. The coupling constant γ_j is the matrix element of the electron-phonon interaction Hamiltonian taken between exciton wave functions. For example, in the case of the piezoelectric coupling whose relevant Hamiltonian is given in (2), the coupling constant is given by

$$\gamma_{l,m,j}=\langle\Phi(\mathbf{r}_e,\mathbf{r}_h)|\sum_{l_e,m_e}\mathcal{P}_{l_e,m_e,l,m,j}(\mathbf{r}_e)Y_{l_e,m_e}(\Omega_e)+\sum_{l_h,m_h}\mathcal{P}_{l_h,m_h,l,m,j}(\mathbf{r}_h)Y_{l_h,m_h}(\Omega_h)|\Phi(\mathbf{r}_e,\mathbf{r}_h)\rangle\,, \tag{6}$$

where $\Phi(\mathbf{r}_e,\mathbf{r}_h)$ is the exciton wave function. The term proportional to γ_j in (5) represents the shift of the origin of the lattice vibration in the excitonic state relative to the ground state and can be interpreted also as representing the adiabatic fluctuation of the excitonic energy level. The homogeneous linewidth due to this fluctuation can be evaluated as [19]

$$\Gamma_h^2(\mathrm{ac})=\sum_j\gamma_j^2[1+2N(\hbar\omega_j)]\,, \tag{7}$$

where N is the phonon occupation number. In the summation over the phonon modes in (7) only the acoustic modes are included because the LO modes have large frequencies and are giving rise to the absorption or emission sidebands rather than causing the energy fluctuation of the excitonic level.

In the high temperature region such that $k_BT\gg\hbar\omega_j$, the T-linear term of Γ_h is proportional to $\sum_j\gamma_j^2/\hbar\omega_j$. The size dependence of this coefficient will be examined. In the case of the deformation-potential coupling, since $\gamma_j\propto 1/R^2$, $\omega_j\propto 1/R$, and the phonon mode density scales as R, we have $\sum_j\gamma_j^2/\hbar\omega_j\propto 1/R^2$. Precisely speaking, the size dependence of the coupling constant γ_j is determined

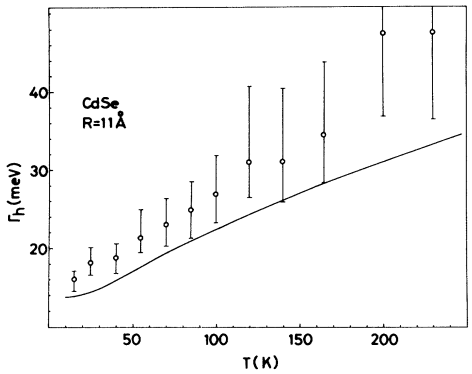

FIG. 1. The pure (adiabatic) dephasing rate of the lowest exciton state in a CdSe nanocrystal with 11 Å radius is plotted as a function of temperature. The experimental data of Ref. [13] are also plotted with error bars.

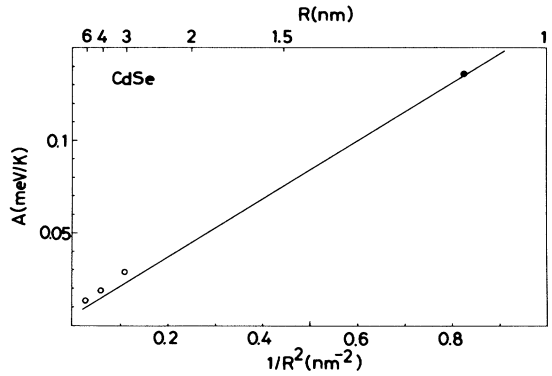

FIG. 2. The coefficient of the linearly temperature-dependent term of the pure dephasing rate in CdSe nanocrystals is plotted as a function of the inverse square of the radius. The solid circle represents the experimental value for an 11 Å radius CdSe nanocrystal (Ref. [13]), while the open circles depict the experimental values for $CdSe_{0.88}S_{0.12}$ nanocrystals with radii of 3, 4, and 6 nm (Ref. [14]).

not only by the electron-phonon interaction Hamiltonian but also by the exciton wave function. However, the gross features can be grasped by the above argument since the size dependence arising from the latter factor is not very strong. In the case of the piezoelectric coupling a similar argument shows that $\sum_j \gamma_j^2/\hbar\omega_j$ is independent of the size. These are the key arguments to clarify the underlying mechanisms of the excitonic dephasing in semiconductor nanocrystals.

Recently, the excitonic dephasing rate in a CdSe nanocrystal with 11 Å radius was measured as a function of the temperature and a typical T-linear dependence was observed, namely, $\Gamma_h = \Gamma_0 + AT + \cdots$, over a wide range of temperature [13]. The theoretically estimated pure dephasing rate of the lowest excitonic state for this nanocrystal is shown in Fig. 1 as a function of temperature with the experimental results [13]. The calculation has been carried out without any adjustable parameter employing the material parameters such as E_d, e_{31}, e_{33}, and e_{15} of bulk CdSe [20] and the exciton wave functions calculated by the method of Ref. [21]. The overall good agreement is obtained between the theory and the experiment except for a constant background ($\sim$3 meV), whose origin will be discussed later briefly. The coefficient A of the T-linear term of Γ_h is plotted in Fig. 2 as a function of $1/R^2$. The linearity to $1/R^2$ is clearly seen, indicating that the deformation-potential coupling is dominantly determining the T-linear term. The experimental value of 0.136 meV/K for an 11 Å radius nanocrystal is reproduced fairly well by the theory. For the sake of reference, the experimental values of A for $CdSe_{0.88}S_{0.12}$ nanocrystals [14] are plotted in Fig. 2 by open circles. Since the material parameters of $CdSe_{0.88}S_{0.12}$ are not much different from those of CdSe in the virtual crystal approximation, we can confirm the characteristic $1/R^2$ dependence of A due to the deformation-potential coupling.

In order to see the relative ratio between contributions from the deformation-potential coupling and the piezoelectric coupling, we decompose (7) as $\Gamma_h^2(\mathrm{ac}) = \Gamma_h^2(\mathrm{DF}) + \Gamma_h^2(\mathrm{PZ})$, where the first (second) term is the contribution from the deformation-potential (piezoelectric) coupling. In Fig. 3 these contributions are plotted as a function of the radius for CdSe nanocrystals at 80 K. As expected before, in the small size region $\Gamma_h^2(\mathrm{DF})$ is overwhelming, whereas in the large size region $\Gamma_h^2(\mathrm{PZ})$ is dominant. The crossover between the two components occurs around $R = 70$ Å.

In CuCl nanocrystals embedded in NaCl matrices, the excitonic dephasing rate was measured systematically as a function of the temperature and the nanocrystal size

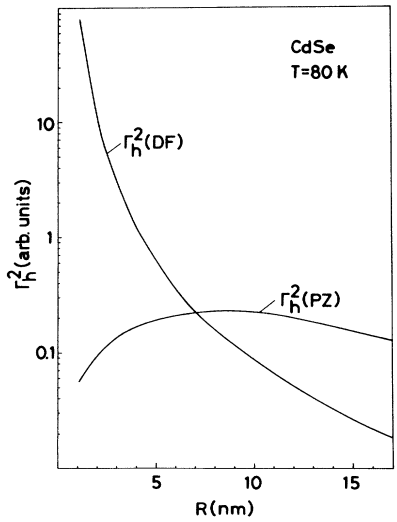

FIG. 3. The squared pure dephasing rate is decomposed into two components $\Gamma_h^2(\mathrm{DF})$ and $\Gamma_h^2(\mathrm{PZ})$ arising from the deformation-potential coupling and the piezoelectric coupling, respectively. These components in CdSe nanocrystals at 80 K are plotted as a function of the radius.

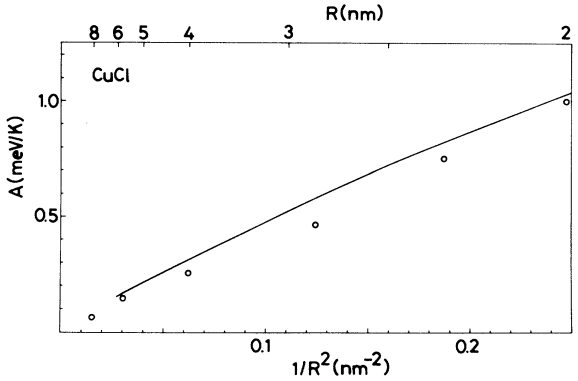

FIG. 4. The coefficient of the linearly temperature-dependent term of the pure dephasing rate in CuCl nanocrystals is plotted as a function of the inverse square of the radius. The open circles represent the experimental values of Ref. [7].

[7]. The size dependence of the coefficient A of the T-linear term of Γ_h was found to be well described by $1/R^2$. The coefficient A is calculated employing the material parameters of bulk CuCl [20] and is shown in Fig. 4 as a function of $1/R^2$ with the experimental data [7]. In this case also the characteristic dependence of A on $1/R^2$ due to the deformation-potential coupling can be confirmed both theoretically and experimentally.

Finally, we will discuss briefly the contribution of the longitudinal relaxation processes to the dephasing constant. As such processes, we can consider phonon-assisted transitions to other excitonic states or to trapped states associated with the nanocrystal surface and defects. In the case of CdSe, the energy splitting between the A and B excitons is very close to an LO phonon energy ($\sim$26 meV) [20] and the LO phonon-assisted transition to the B exciton is expected to contribute significantly to the dephasing rate of the A exciton at high temperatures. In fact, the deviation of the theoretical pure dephasing rate in Fig. 1 from the experimental value at high temperatures (>200 K) can be explained by this mechanism. The localized excitonic states associated with the surface or defects were found more than several tens of meV below the lowest excitonic state [22]. Thus the transitions to those states occur through multiphonon emission and contribute an almost temperature-independent term to the excitonic dephasing rate giving rise to a constant background which persists even at $T=0$ K. The almost constant ($\sim$3 meV) deviation of the theoretical pure dephasing rate from the experimental value in Fig. 1 below $\sim$100 K can be explained by this mechanism. However, quantitative estimate of these longitudinal relaxation rates is left for future study.

In summary, the electron-phonon interactions in semiconductor nanocrystals, especially concerning the acoustic phonon modes, are derived and the size dependence of the contribution to the excitonic dephasing rate has been clarified for various electron-phonon coupling mechanisms. On the basis of these results, the commonly observed linearly temperature-dependent term of the excitonic dephasing rate and the proportionality of its magnitude to the inverse square of the nanocrystal size are attributed to the pure dephasing due to the deformation-potential coupling.

The author is grateful to C. Flytzanis for enlightening discussions at the initial stage of this study. He would also like to thank N. Uesugi, J. Yumoto, and H. Shinojima for many valuable discussions.

[1] L. E. Brus, Appl. Phys. A **53**, 465 (1991); M. G. Bawendi, M. L. Steigerwald, and L. E. Brus, Annu. Rev. Phys. Chem. **41**, 477 (1990).
[2] C. Flytzanis, F. Hache, M. C. Klein, D. Ricard, and P. Roussignol, *Progress in Optics,* edited by E. Wolf (Elsevier, Amsterdam, 1991), Vol. XXIX, p. 321.
[3] A. P. Alivisatos, T. D. Harris, P. J. Carroll, M. L. Steigerwald, and L. E. Brus, J. Chem. Phys. **90**, 3463 (1989).
[4] M. C. Klein, F. Hache, D. Ricard, and C. Flytzanis, Phys. Rev. B **42**, 11 123 (1990).
[5] A. Tanaka, S. Onari, and T. Arai, Phys. Rev. B **45**, 6587 (1992).
[6] A. Tanaka, S. Onari, and T. Arai, Phys. Rev. B **47**, 1237 (1993).
[7] T. Itoh and M. Furumiya, J. Lumin. **48&49**, 704 (1991).
[8] T. Wamura, Y. Masumoto, and T. Kawamura, Appl. Phys. Lett. **59**, 1758 (1991).
[9] N. Peyghambarian, B. Fluegel, D. Hulin, A. Migus, M. Joffre, A. Antonetti, S. W. Koch, and M. Lindberg, IEEE J. Quantum Electron. **25**, 2516 (1989).
[10] P. Roussignol, D. Ricard, C. Flytzanis, and N. Neuroth, Phys. Rev. Lett. **62**, 312 (1989).
[11] M. G. Bawendi, W. L. Wilson, L. Rothberg, P. J. Carroll, T. M. Jedju, M. L. Steigerwald, and L. E. Brus, Phys. Rev. Lett. **65**, 1623 (1990).
[12] U. Woggon, S. Gaponenko, W. Langbein, A. Uhrig, and C. Klingshirn, Phys. Rev. B **47**, 3684 (1993).
[13] R. W. Schoenlein, D. M. Mittleman, J. J. Shiang, A. P. Alivisatos, and C. V. Shank, Phys. Rev. Lett. **70**, 1014 (1993).
[14] H. Shinojima, J. Yumoto, T. Takagahara, and N. Uesugi, in Proceedings of the Quantum Electronics and Laser Science Conference, Baltimore, 1993 (to be published), QWH26.
[15] A. E. H. Love, *A Treatise on the Mathematical Theory of Elasticity* (Dover, New York, 1944).
[16] H. Lamb, Proc. Math. Soc. London **13**, 187 (1882).
[17] G. L. Bir and G. E. Pikus, *Symmetry and Strain-Induced Effects in Semiconductors* (Wiley, New York, 1974).
[18] W. G. Cady, *Piezoelectricity* (McGraw-Hill, New York, 1946).
[19] S. Nakajima, Y. Toyozawa, and R. Abe, *The Physics of Elementary Excitations* (Springer-Berlin, 1980).
[20] *Physics of II-VI and I-VII Compounds*, edited by O. Madelung, M. Schulz, and H. Weiss, Landolt-Börnstein, New Series, Group 3, Vol. 17, Pt. b (Springer, Berlin, 1982).
[21] T. Takagahara, Phys. Rev. B **47**, 4569 (1993).
[22] F. Hache, M. C. Klein, D. Ricard, and C. Flytzanis, J. Opt. Soc. Am. B **8**, 1802 (1991).